

THE ORIGIN OF STEEP VERTICAL STELLAR DISTRIBUTION IN THE GALACTIC DISK

ARUNIMA BANERJEE AND CHANDA J. JOG

Department of Physics, Indian Institute of Science, Bangalore 560012, India;
arunima_banerjee@physics.iisc.ernet.in, cjog@physics.iisc.ernet.in

Received 2007 January 17; accepted 2007 March 3

ABSTRACT

Over the past two decades, observations have revealed that the vertical density distribution of stars in galaxies near the midplane is substantially steeper than the sech^2 function that is expected from an isothermal approximation. However, the physical origin for this has not been explained so far. Here we show that such steep profiles result naturally, even within the isothermal regime, on taking into account the gravitational force due to the gas. Because of its low velocity dispersion, the gas is concentrated closer to the Galactic midplane than the stars, and hence it strongly affects the vertical stellar distribution, even though its contribution to the total surface density is small. We apply a three-component Galactic disk model consisting of gravitationally coupled stars and H I and H₂ gas embedded in the dark matter halo, and calculate the vertical density distribution of stars for the Galaxy. The resulting vertical density distribution of stars is shown to be steeper than the sech^2 function, lying between the sech^2 and an exponential function, in good agreement with observations of galaxies. We also show that a multicomponent stellar disk consisting of coupled dwarfs and two populations of giants does not explain the observed steep stellar profiles.

Subject headings: galaxies: ISM — galaxies: kinematics and dynamics — galaxies: photometry — galaxies: structure — Galaxy: structure — hydrodynamics

1. INTRODUCTION

It is well known that a gravitating, isothermal stellar disk in a galaxy can be represented by a self-consistent vertical distribution that obeys a sech^2 profile, as has been shown theoretically (Spitzer 1942) and confirmed by observations (van der Kruit & Searle 1981a, 1981b). However, recent studies have shown that the observed vertical distribution in galaxies is steeper and is well approximated by an exponential or a sech function, especially close to the galactic midplane, as shown for our Galaxy (Gilmore & Reid 1983; Pritchett 1983; Kent et al. 1991; Gould et al. 1996) and also for external galaxies (Wainscoat et al. 1989; Aoki et al. 1991; Barnaby & Thronson 1992; van Dokkum et al. 1994; Rice et al. 1996). These later, near-infrared observations, which are free from the errors due to dust extinction, allow one to probe regions closer to the midplane. These show an excess over the isothermal case near the midplane, which is better fitted by an exponential or a sech profile.

The sech^2 profile results under the isothermal assumption for the equation of state, so that the pressure p can be written as density ρ times the square of the sound velocity or the random velocity dispersion, and the additional assumption that the velocity dispersion is independent of vertical distance (Spitzer 1942; Bahcall 1984). An exponential distribution, as observed in some cases, was argued to be unphysical when extended all the way to the midplane, and a fit intermediate between an exponential and an isothermal was suggested in terms a family of curves denoted by a parameter n (van der Kruit 1988). Subsequent observational papers analyze the data and give their results in terms of this parameter n (see, e.g., de Grijs & van der Kruit 1996; de Grijs et al. 1997). However, the set of models proposed by van der Kruit (1988) is somewhat ad hoc, since it is not obtained as a solution to the basic equations relevant in this context.

The physical origin of the steeper-than-isothermal vertical profile has not been fully explained so far. An exponential profile is shown to result if the gas settles in a protogalaxy into isothermal equilibrium and if the star formation rate is equal to the cooling rate of the gas (Burkert & Yoshii 1996). However, this model requires a specific set of initial conditions and does not take account

of the secular heating (e.g., Binney & Tremaine 1987) that stars undergo, and also it cannot explain the sech behavior seen in many galaxies.

In this paper, we show that the steep vertical profile occurs naturally on taking account of the strong constraining effect of the gravitational force due to gas. Because of its lower velocity dispersion, the gas forms a thin layer and thus lies closer to the galactic midplane than the stars; hence, despite its small mass fraction, the inclusion of gas is shown to significantly affect the stellar vertical distribution. We apply a three-component model of a galactic disk consisting of gravitationally coupled stars and H I and H₂ gas in the field of a dark matter halo, developed earlier by Narayan & Jog (2002b). The resulting thickness was defined as the HWHM of the vertical distribution for each component, and it showed a good agreement with observations for the inner Galaxy (Narayan & Jog 2002b), and the moderate stellar flaring predicted also agreed well with observations of external galaxies (Narayan & Jog 2002a). In the current paper, we concentrate on the density distribution close to the midplane. There is no discrepancy in these two approaches, since at higher vertical distances, the various functional forms have the same (sech^2) behavior. We treat the stellar disk as a single component for simplicity; this assumption is justified later.

The results obtained in this paper show that the inclusion of gas gravity can account for the observed steepness in the stellar profiles closer to the midplane. Also, we predict the surface-brightness distribution in the K band at different galactocentric radii within the Galaxy, considering it as an edge-on system as it would appear to an external observer.

In § 2, we discuss the model used and the method for solving the equations and give the parameters used. Section 3 contains the results obtained, and §§ 4 and 5 give the discussion and the conclusion, respectively.

2. FORMULATION OF EQUATIONS AND SOLUTIONS

We have used the three-component galactic disk model of Narayan & Jog (2002b) to obtain the vertical density distribution of stars in the Galaxy, as discussed in § 1. In this model, the

response of each component to the joint potential determines the net vertical density distribution in a self-consistent manner. The atomic and molecular hydrogen gas are distributed in two thin disks, embedded within the stellar disk, with which they are also axisymmetric and coplanar. We use the galactic cylindrical coordinates (R, ϕ, z) . The equation of hydrostatic equilibrium in the vertical direction is given by (Rohlf's 1977)

$$\frac{\langle (v_z)_i^2 \rangle}{\rho_i} \frac{d\rho_i}{dz} = (K_z)_s + (K_z)_{H_1} + (K_z)_{H_2} + (K_z)_{DM}, \quad (1)$$

where $i = 1, 2, 3$, and DM denote these quantities for stars, H I and H₂ gas, and the dark matter halo, respectively. Here $K_z = -\partial\psi/\partial z$ is the force per unit mass along z , ψ is the corresponding potential, and $\langle (v_z)_i^2 \rangle^{1/2}$ is the random velocity dispersion along z . We have assumed the equation of state to be isothermal and the dispersion to be constant with z .

Under the assumption of a thin disk, the joint Poisson equation simplifies to

$$\frac{d^2\psi_s}{dz^2} + \frac{d^2\psi_{H_1}}{dz^2} + \frac{d^2\psi_{H_2}}{dz^2} = 4\pi G(\rho_s + \rho_{H_1} + \rho_{H_2}). \quad (2)$$

On combining equations (1) and (2), the density distribution of a component i at any radius is given by

$$\frac{d^2\rho_i}{dz^2} = \frac{\rho_i}{\langle (v_z)_i^2 \rangle} \left[-4\pi G(\rho_s + \rho_{H_1} + \rho_{H_2}) + \frac{d(K_z)_{DM}}{dz} \right] + \frac{1}{\rho_i} \left(\frac{d\rho_i}{dz} \right)^2. \quad (3)$$

From the above equation, it is evident that although there is a common gravitational potential, the response of each component will be different due to the difference in their random velocity dispersions.

2.1. Solution of the Equations

The above equation represents a set of three coupled, second-order ordinary differential equations, which is solved numerically by the fourth-order Runge-Kutta method in an iterative fashion (Narayan & Jog 2002b), with the following two initial conditions at the midplane, i.e., $z = 0$ for each component:

$$\rho_i = (\rho_0)_i, \quad \frac{d\rho_i}{dz} = 0. \quad (4)$$

However, the modified midplane density $(\rho_0)_i$ for each component is not known a priori. Instead, the net surface density $\Sigma_i(R)$, given by twice the area under the curve of $\rho_i(z)$ versus z , is used as the second boundary condition, since this is known observationally. Hence the required value of $(\rho_0)_i$ can be determined by a trial and error method, which eventually fixes the $\rho_i(z)$ distribution.

2.2. Parameters Used

We require the surface density and the velocity dispersion for each component to solve the coupled set of equations at each radius; these parameters have been taken as in Narayan & Jog (2002b). The observed values were used for the gas surface densities (Scoville & Sanders 1987); see Table 1. The stellar surface density and the density profile of the dark matter halo were taken from the standard mass model for the Galaxy by Mera et al. (1998): here the stellar disk has an exponential distribution with a disk scale length of 3.2 kpc and local stellar density of $45 M_\odot \text{pc}^{-2}$,

TABLE 1
BEST-FITTING $2/n$ VALUES AT DIFFERENT RADII

Radius (kpc)	Σ_{H_1} ($M_\odot \text{pc}^{-2}$)	Σ_{H_2} ($M_\odot \text{pc}^{-2}$)	$\Sigma_{H_1+H_2}/\Sigma_s$	n	$2/n$
2.....	1.8	4.0	0.02	3.33	0.6
3.....	3.8	4.9	0.04	5.4	0.37
4.....	4.6	13.1	0.10	7.32	0.27
4.5.....	4.6	19.7	0.16	9.12	0.22
5.....	4.6	14.2	0.14	7.91	0.25
6.....	4.6	10.8	0.16	6.89	0.29
7.....	4.7	4.9	0.13	4.86	0.41
8.....	5.3	3.6	0.17	4.5	0.44
8.5.....	5.6	2.1	0.17	4.26	0.47
9.....	5.6	1.4	0.18	4.22	0.47
10.....	5.6	0.8	0.23	2.93	0.68
11.....	5.6	0.6	0.30	2.88	0.69
12.....	5.6	0.4	0.40	2.83	0.71

which gives a central stellar surface density of $641 M_\odot \text{pc}^{-2}$, and the dark matter halo is taken as an isothermal sphere with a core radius of 5 kpc and a rotation velocity of 220km s^{-1} . Table 1 also lists the values of the ratio $\Sigma_{H_1+H_2}/\Sigma_s$, the total gas to stellar surface mass density.

The observed gas velocity dispersion values are taken, with 8km s^{-1} for H I (Spitzer 1978) and 5km s^{-1} for H₂ gas (Stark 1984; Clemens 1985). The observed planar stellar velocity dispersion values from Lewis & Freeman (1989) were used to obtain the vertical dispersion values, assuming the same ratio, namely 1/2, of the velocity dispersions as seen in the solar neighborhood (Binney & Merrifield 1998). This gives an exponential velocity distribution with a scale length of 8.7 kpc and local value of 18km s^{-1} (Lewis & Freeman 1989; Narayan & Jog 2002b).

3. RESULTS

3.1. Effect of Gas on Stellar Vertical Distribution

We first illustrate the dynamical effect of the inclusion of the low-dispersion component, namely the gas, on the vertical distribution of stars. We first compare the gravitational force due to stars and gas taken separately. The strength of the force per unit mass, $|K_z|$, for an isothermal single component is obtained by solving the force equation and the Poisson equation (eqs. [1] and [2]) together. These can be solved analytically and give (Spitzer 1942; Rohlf's 1977)

$$|K_z| = 2 \frac{\langle v^2 \rangle}{z_0} \tanh(z/z_0), \quad (5)$$

where $\langle v^2 \rangle$ is the mean square of the velocity. The vertical density distribution is given by

$$\rho(z) = \rho_0 \text{sech}^2(z/z_0), \quad (6)$$

where the constant z_0 is given in terms of the midplane density, ρ_0 , as

$$z_0 = \left[\frac{\langle v^2 \rangle}{2\pi G \rho_0} \right]^{1/2}. \quad (7)$$

We treat the stars-alone case first and use the total observed stellar surface density Σ_s at a given radius as a boundary condition; integrating equation (6), we constrain both ρ_0 and z_0 simultaneously. The procedure is then repeated for the gas-alone H I and H₂

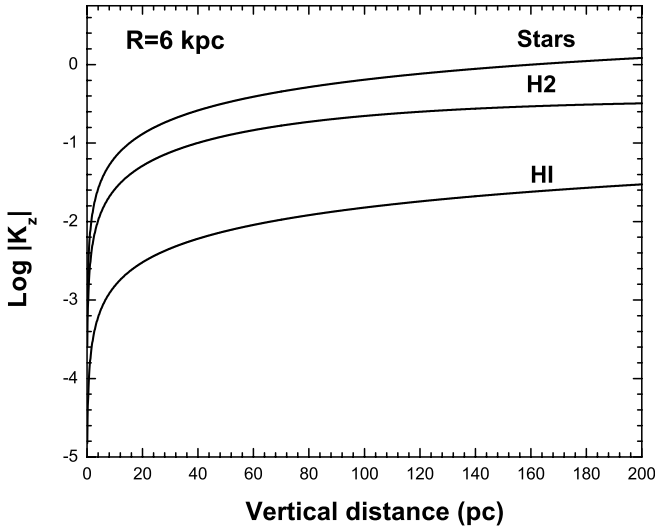


FIG. 1.—Plot of force per unit mass $|K_z|$ for the stars-alone case and the H_2 -alone and $H\text{I}$ -alone cases on a log scale vs. z , calculated at $R = 6$ kpc. The force due to the gas is a significant fraction, $\sim 30\%$ of the stars-alone case for z -values close to the Galactic midplane ($z \leq 150$ pc).

components taken separately. The resulting values for $|K_z|$, the strength of the force per unit mass due to stars alone, and that due to $H\text{I}$ and H_2 alone (drawn on a log scale) versus z are shown in Figure 1, as calculated at $R = 6$ kpc. It is clear that up to $|z| < 150$ pc, the force due to gas is significant: $\sim 30\%$ of that due to stars. This is the spatial region over which we have fitted the $n(z)$ profiles to obtain the parameter n (§ 3.2). Thus, we expect to see a steepening of the density profile of stars on taking account of the gas gravity.

A similar plot for the coupled case cannot be given, since the three disk components (stars, $H\text{I}$, and H_2) are coupled, and hence the individual terms on the right-hand side of equation (1) are not known. However, a gradient of K_z with z can be given in terms of the mass density, ρ , for each component, using the Poisson equation. The resulting values of mass densities for the three coupled components as obtained from our model at $R = 6$ kpc are plotted in Figure 2. This is another indicator of the importance of gas in the dynamics close to the midplane. The midplane density of the gas and the stars are comparable, hence the gas gravity affects the stellar dynamics significantly.

The dynamical effect of gas gravity on the net vertical density distribution of stars is clearly shown in Figure 3, where we plot and compare the stellar density distribution versus z for the stars-alone case and also as obtained in the coupled system. First, the central or the midplane peak in density is increased, and the shape of the central profile becomes sharper, which is studied quantitatively in terms of the parameter “ n ” in the rest of the paper. Furthermore, the scale height (HWHM) of the stellar distribution is lower in the coupled system due to the inclusion of gas gravity—this aspect was studied in detail in our earlier work (Narayan & Jog 2002b). Thus the inclusion of gas affects the central peak density of the stellar distribution and the shape of the profile, and it also decreases the stellar vertical scale height.

We have thus shown that due to its lower velocity dispersion, the gas forms a thinner layer and is concentrated closer to the galactic midplane than the stars. Hence, despite the fact that the gas contains a small fraction of the total disk surface density, it has a significant effect on the vertical density distribution of the main mass component, namely, the stars.

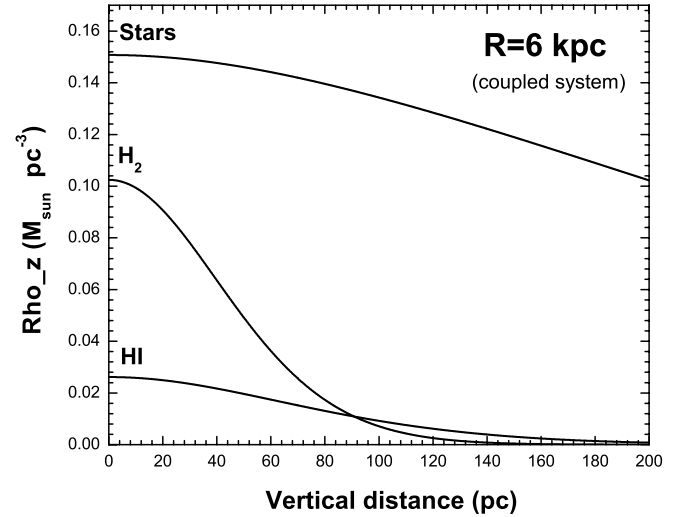


FIG. 2.—Density distribution vs. z for the gravitationally coupled three-component system obtained at $R = 6$ kpc, plotted for the stars, H_2 , and $H\text{I}$ gas components. The gas density is a significant fraction of the stellar density close to the midplane, and hence the force due to gas has a strong effect on the stellar distribution, despite the fact that the gas surface density is a small fraction of the total disk surface density.

A study highlighting a similar constraining effect of a molecular cloud complex was done by Jog & Narayan (2001). The cloud complex is massive ($\sim 10^7 M_\odot$) and extended (~ 200 pc in size), with an average density much higher than the midplane stellar density, and hence in that case the $|K_z|$ due to the complex dominates the $|K_z|$ due to the stars-alone case (Fig. 1 in that paper), and the resulting changes in the vertical density distribution of stars and the HWHM (Figs. 3 and 4, respectively, in that paper) are much stronger. Figures 1 and 3 in that paper are the analogs of Figures 1 and 3 given above.

3.2. Model Stellar Vertical Profiles

The self-consistent vertical density distribution of stars was determined for the radial range of 2–12 kpc in the Galaxy, following the method discussed in § 2.1. In order to compare our results with

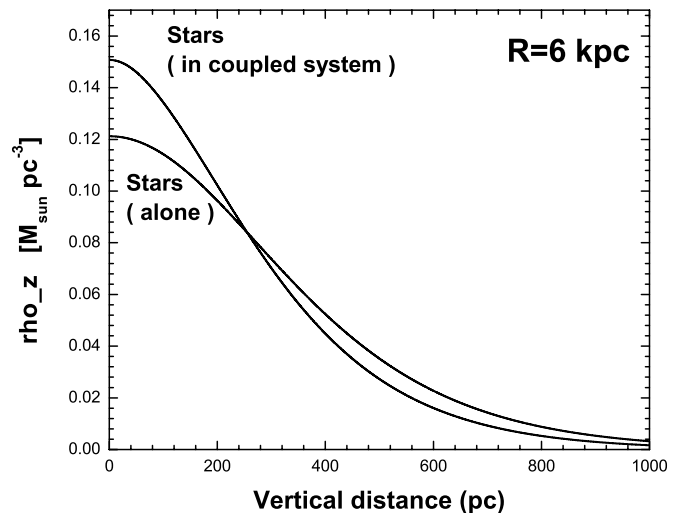


FIG. 3.—Density distribution vs. z for the stars-alone case and for the stars in a gravitationally coupled three-component system obtained at $R = 6$ kpc. Because of the gravitational force due to gas, the stellar distribution in the coupled case has a higher central value, the profile is steeper, and the thickness (HWHM) is smaller.

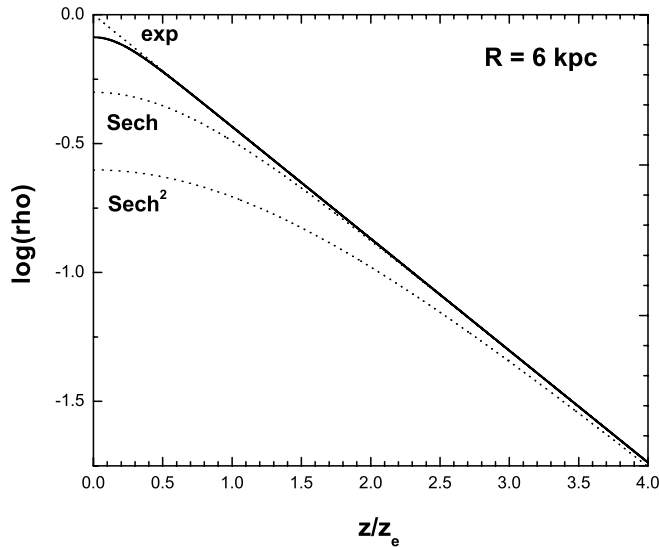


FIG. 4.—Plot of vertical density distribution vs. z/z_e , at $R = 6$ kpc. The model profile (solid line) is best fitted by the $n = 6.9$ case from van der Kruit (1988), is steeper than the stars-alone isothermal or the sech^2 cases ($n = 1$), and lies between the $\text{sech} z$ ($n = 2$) case and an exponential ($n = \infty$) case (dotted lines). This region lies within the molecular ring of high gas density, hence it results in a steep vertical profile.

the observational papers in the literature which have fitted their data to the van der Kruit (1988) curves, we also fit our numerical solution for $\rho(z)$, the stellar mass density, to the family of curves suggested by van der Kruit (1988),

$$\rho(z) = 2^{-2/n} \rho_e \text{sech}^{2/n}(nz/2z_e), \quad (8)$$

which is characterized by three parameters, ρ_e , z_e , and n . Here ρ_e is the extrapolated outer mass density away from the galaxy plane, which is the same for all values of n at large z , and z_e is the vertical scale parameter. For a given ρ_e , the effective scale heights and the amplitudes at $z = 0$ are obtained as a function of the parameter n .

In the limiting cases of $n = 1$ and $n = \infty$, equation (8) reduces to the usual isothermal (or the sech^2 function) and exponential functions, respectively, while $n = 2$ denotes an intermediate case of the sech profile.

In Figures 4 and 5, we compare the vertical stellar-density profiles for the $n = \infty$ (exp), $n = 2$ (sech), and $n = 1$ (sech^2) cases with our model curves obtained at $R = 6$ kpc and 8.5 kpc, respectively. The values of the parameters ρ_e and z_e in these cases are the best-fitting values obtained from fitting our model curves to within $|z| \leq 150$ pc of the galactic midplane. The model curve in Figures 4 and 5 is best fitted by $n = 6.9$ and $n = 4.3$, respectively, and it thus lies between the sech and an exponential profile. In the region of the molecular ring, which includes $R = 6$ kpc, the influence of gas is higher, and hence the resulting vertical profile is steeper than in the solar neighborhood region of 8.5 kpc. This underlines the crucial effect of gas in causing a steepening of the vertical stellar density profile in the galactic disk. The best-fit values for z_e are 368 pc and 362 pc. From these figures, it is clear that the best-fitting value of n depends on the range of z used, and at a large enough z -range, all curves go over to the usual sech^2 profile.

The effect of gas gravity is further illustrated by plotting the best-fitting $2/n$ values versus radius for the Galaxy, obtained from our analysis in Figure 6. Also, Table 1 gives the best-fitting $2/n$ values obtained at different radii, along with the total gas fraction

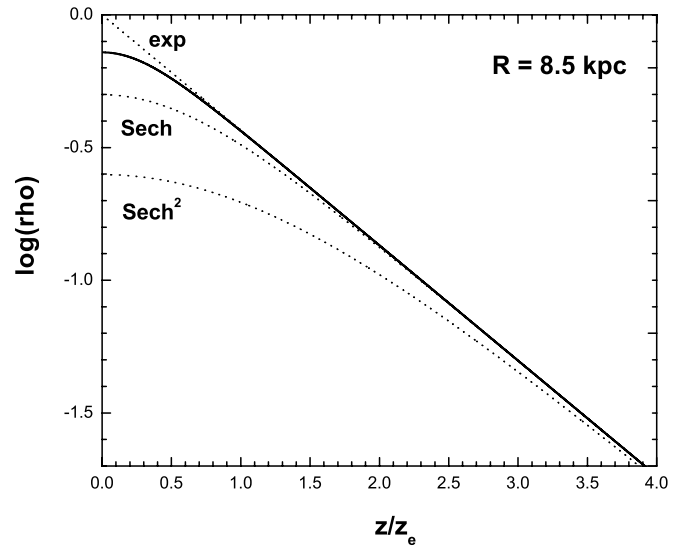


FIG. 5.—Plot of vertical density distribution vs. z/z_0 , at $R = 8.5$ kpc. The vertical model profile is best fitted by the $n = 4.3$ case from van der Kruit (1988), which is closer to the sech case and is less sharp than at $R = 6$ kpc, but is still sharper than the stars-alone, isothermal case ($\text{sech}^2 z$).

at each radius. It shows that $2/n$ lies between 0 and 1 in general, or that n lies between ∞ and 2. Thus, our model vertical distribution is steeper than the one-component isothermal case ($n = 1$) at all radii, and lies between an exponential and a sech profile. This is in direct conformity with the results obtained by de Grijs et al. (1997) for a complete sample of external, edge-on galaxies.

Interestingly, the best-fitting steepness index n is more directly dependent on the total absolute gas surface density than on the gas fraction (see Table 1). This needs to be studied for other galaxy types and gas mass ranges in a future paper.

3.3. Luminosity Profile of a Multicomponent Stellar Disk

So far we have treated the stars as consisting of a single, isothermal component, and our dynamical model gives the steep vertical density profile for this single stellar component when

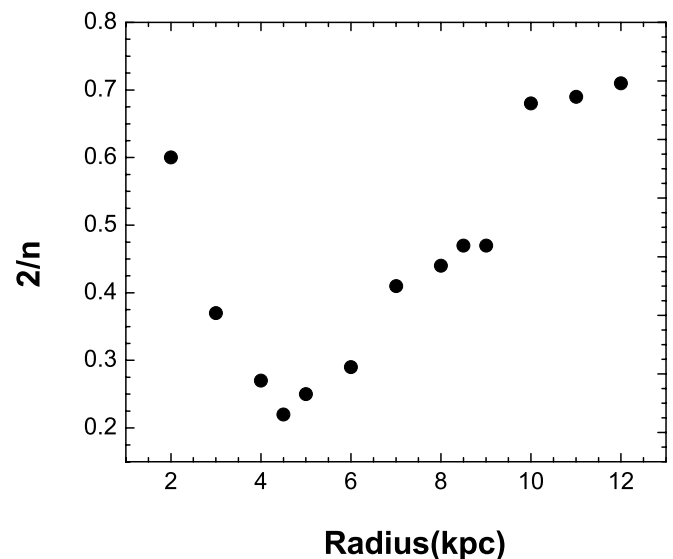


FIG. 6.—Plot of the best-fitting $2/n$ values vs. the radius of 2–12 kpc for the Galaxy, where n is the van der Kruit parameter denoting the steepness of the stellar vertical profile.

coupled with the H I and H₂ gas components. We confirm the validity of this assumption next.

Alternatively, a steepening of the stellar vertical luminosity profile could also occur if a superposition of stellar components with different velocity dispersions is considered, as has been suggested qualitatively (de Grijs et al. 1997). We check and refute this idea by considering a coupling of the G-K-M dwarfs which contain the main mass fraction in the stellar disk, and giants which contain a much smaller disk mass fraction but dominate the disk luminosity. This latter feature is well known, namely, that the luminosity of the disk is dominated by giants which may not determine its dynamics, as cautioned by Mihalas & Binney (1981). The giants span a large range of velocities, covering a factor of 2, and at first glance it may seem as though that would result in a nonisothermal stellar luminosity profile, or a profile steeper than sech^2 . However, as we show next, the net dynamics in a disk consisting of coupled dwarfs and giants is largely determined by the dwarfs, because they constitute the main disk mass component and the two have comparable dispersions.

We treat the giants as consisting of two separate components or populations characterized by vertical dispersions of 14 km s^{-1} and 28 km s^{-1} , respectively, with 23% of the mass surface density of the giants in the higher velocity component, as was shown in a recent study by Holmberg & Flynn (2004) based on *Hipparcos* data. We then apply our coupled, three-component disk model to the G-K-M dwarfs (treated as a single component) and the above two giant components. The total surface densities of dwarfs and giants are taken to be 13.5 and $0.19 M_{\odot} \text{ pc}^{-2}$, respectively, as observed; see Table 4-16 in Mihalas & Binney (1981).

The resulting net stellar density distribution from our model is fitted by the van der Kruit (1988) function to obtain the “ n ” parameter. Our dynamical model gives the n value for dwarfs in this case to be 1.01, which is almost identical to a one-component sech^2 profile (which is given by $n = 1$). For each of the two populations of giants, the best-fit n value is also 1.01. Next, we add the density profiles for these two giant populations, and the best-fit value for n in this case is found to be 1.07, which is still close to the isothermal case, although it is very slightly steeper than the profile for the individual components. The net luminosity profile, as set by the sum of the giant populations, will thus be nearly sech^2 , or close to isothermal. This is a somewhat surprising result, and physically this can be explained by the fact that the high-velocity giant population has a much lower surface density, hence in the coupled three-component system treated here, its density contribution within 150 pc (this is the z -range over which the fitting for n is done) is much smaller than the other giant component. This is why despite the two giant populations having such different vertical velocity dispersions, the net density profile of the giants is close to that of a single isothermal profile. The n for the combined giants is thus very similar to the n for the main mass component, namely, the dwarfs.

Note that the observed stellar luminosity profile is much steeper, with $n = 2$ or higher; that is, it lies between a sech and an exponential profile (§ 3.2). Thus, a multicomponent stellar disk with observed parameters for the dwarfs and the giants cannot explain the steep light distribution seen in galaxies. In contrast, the inclusion of gas in our model, despite its small mass fraction, naturally results in the steep stellar profile as observed, as shown in § 3.2.

This calculation also confirms that our assumption of a single-component stellar disk is valid for the dynamical study, since the giants do not affect the dynamics of dwarfs. Similarly, even in the coupled stars-gas case treated in our paper, the luminosity profile of the giants at low z can be taken to trace that of the main stellar-mass component, namely, the dwarfs.

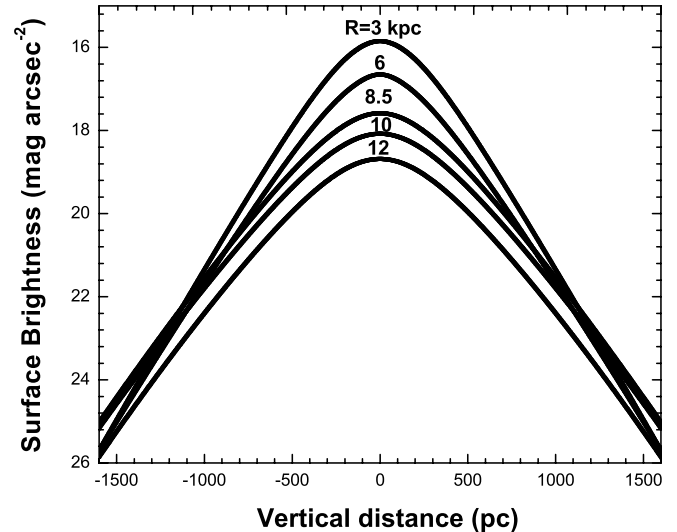


FIG. 7.—Plot showing the model surface-brightness curves in the K band vs. the distance z from the midplane, calculated at different galactocentric radii, treating the Galaxy as an edge-on system as seen by an external observer.

3.4. Model Surface Brightness versus Height z

The luminosity density of stars in a particular color band is the directly observed quantity in astronomy, rather than mass density itself. But as the luminosity density in any color band is taken to be a constant multiple of the stellar density function, we conclude that the vertical luminosity distribution follows the same functional form as the corresponding mass density distribution, and hence is characterized by the same value of the steepness index n .

We next obtain the surface brightness distribution of a typical edge-on galaxy like the Milky Way, as seen by an external observer, by integrating the luminosity density function along a line of sight. If the luminosity density at a galactocentric radius R and vertical distance z above the midplane is given by (see van der Kruit & Searle 1981a)

$$L(R, z) = L_0 \text{sech}^{2/n}(nz/2z_e) \exp(-R/h), \quad (9)$$

where h is the disk scale length, then the surface brightness is given by

$$I(R, z) = I(0, 0)(R/h)K_1(R/h) \text{sech}^{2/n}(nz/2z_e), \quad (10)$$

where $I(0, 0) = 2L_0h$ and K_1 is the modified Bessel function. If $I(R, z)$ is in units of $L_{\odot} \text{ pc}^{-2}$, the surface brightness in units of magnitude per arcsec² is (Binney & Merrifield 1998)

$$\mu(R, z) = -2.5 \log(I/L_{\odot} \text{ pc}^{-2}) + M_{\odot} + 21.572. \quad (11)$$

Here M_{\odot} denotes the absolute solar magnitude in the chosen color band. For the K band, $M_{\odot} = 3.33$ (Cox 2000), and the above formula reduces to

$$\mu(R, z) = -2.5 \log(I/L_{\odot} \text{ pc}^{-2}) + 24.902. \quad (12)$$

Our Galaxy is known to have an exponential disk (e.g., Mera et al. 1998) with an exponential luminosity profile as given in equation (9); from this we obtain the surface-brightness profiles in the K band at a given radius as follows. The stellar density value at each z (in units of $M_{\odot} \text{ pc}^{-3}$) at a given R obtained from our numerical analysis is divided by M_{\odot}/L_{\odot} of 1 to obtain the corresponding

luminosity density in the K band in units of $L_{\odot} \text{pc}^{-3}$. This ratio of mass-to-luminosity is obtained using the K -band disk luminosity from Kent et al. (1991) and the disk mass from Binney & Tremaine (1987), and is in agreement with a study based on a large number of galaxies (Bell & de Jong 2001) which has shown the typical value of this ratio to be ~ 0.5 , with a scatter of a few around it. Then, using equations (10) and (11), we obtain the surface-brightness distribution at a given radius. In Figure 7, we plot the model surface-brightness distribution in the K band, calculated at different radii, treating the Milky Way as an edge-on system as seen by an external observer. These curves are strikingly similar to the observed profiles for external edge-on galaxies (see Fig. 3 from Barteldrees & Dettmar 1994, and Fig. 5 from de Grijs et al. 1997).

4. DISCUSSION

1. We have assumed the stellar disk to be isothermal for simplicity, as is the standard practice in the study of the vertical structure of galactic disks (e.g., Spitzer 1942; Bahcall 1984). The stellar velocity dispersion increases due to secular heating by tidal interactions and molecular clouds (e.g., Binney & Tremaine 1987). Despite this, the resulting stellar vertical velocity dispersion is shown to be constant with height (Jenkins & Binney 1990; Jenkins 1992), hence the isothermal assumption made is robust.

2. The model developed here is general, and since the gas velocity dispersion in external galaxies is universally much smaller than the stellar dispersion (see, e.g., Lewis 1984; Wilson & Scoville 1990), the analysis in this paper can be applied to other galaxies as well. We predict that gas-rich late-type galaxies will

show steeper stellar profiles (higher n or lower $2/n$ values) than early-type galaxies for the same radial range. This could be checked with future observations.

5. CONCLUSION

It is well established that the vertical distribution of stars in galactic disks is observed to be steeper than the sech^2 profile expected from a one-component, isothermal case, especially closer to the galactic midplane. In this paper, we provide a simple, physical origin for this: we show that on taking account of the gas gravity, the resulting stellar vertical profile, even under the isothermal assumption, is steeper than the sech^2 function. The resulting profile is calculated for our Galaxy using a three-component model of a galactic disk consisting of gravitationally coupled stars and gas, and is shown to be steeper than sech^2 , lying between a sech profile and an exponential profile, in agreement with observations of galaxies. The higher the gas surface density, the steeper the resulting stellar vertical profile, asymptotically approaching the exponential curve. Due to the lower velocity of gas, it is concentrated close to the midplane, and this crucial feature results in the steepening of the stellar profile. We also show that the observed steep stellar profiles cannot be explained by a superposition of several stellar components, as has sometimes been proposed qualitatively in the literature.

We thank the anonymous referee for insightful comments which have improved our paper.

REFERENCES

- Aoki, T. E., Hiromoto, N., Takami, H., & Okamura, S. 1991, PASJ, 43, 755
 Bahcall, J. N. 1984, ApJ, 276, 169
 Barnaby, D., & Thronson, H. A., Jr. 1992, AJ, 103, 41
 Barteldrees, A., & Dettmar, R.-J. 1994, A&AS, 103, 475
 Bell, E. F., & de Jong, R. S. 2001, ApJ, 550, 212
 Binney, J., & Merrifield, M. 1998, Galactic Astronomy (Princeton: Princeton Univ. Press)
 Binney, J., & Tremaine, S. 1987, Galactic Dynamics (Princeton: Princeton Univ. Press)
 Burkert, A., & Yoshii, Y. 1996, MNRAS, 282, 1349
 Clemens, D. P. 1985, ApJ, 295, 422
 Cox, A. N., ed. 2000, Astrophysical Quantities (New York: Springer)
 de Grijs, R., Peletier, R. F., & van der Kruit, P. C. 1997, A&A, 327, 966
 de Grijs, R., & van der Kruit, P. C. 1996, A&AS, 117, 19
 Gilmore, G., & Reid, N. 1983, MNRAS, 202, 1025
 Gould, A., Bahcall, J. N., & Flynn, C. 1996, ApJ, 465, 759
 Holmberg, J., & Flynn, C. 2004, MNRAS, 352, 440
 Jenkins, A. 1992, MNRAS, 257, 620
 Jenkins, A., & Binney, J. J. 1990, MNRAS, 245, 305
 Jog, C. J., & Narayan, C. A. 2001, MNRAS, 327, 1021
 Kent, S. M., Dame, T. M., & Fazio, G. 1991, ApJ, 378, 131
 Lewis, B. M. 1984, ApJ, 285, 453
 Lewis, J. R., & Freeman, K. C. 1989, AJ, 97, 139
 Mera, D., Chabrier, G., & Schaeffer, R. 1998, A&A, 330, 953
 Mihalas, D., & Binney, J. 1981, Galactic Astronomy (San Francisco: Freeman)
 Narayan, C. A., & Jog, C. J. 2002a, A&A, 390, L35
 ———. 2002b, A&A, 394, 89
 Pritchett, C. 1983, AJ, 88, 1476
 Rice, W., Merrill, K. A., Gatley, I., & Gillett, F. C. 1996, AJ, 112, 114
 Rohlfs, K. 1977, Lectures on Density Wave Theory (Berlin: Springer)
 Scoville, N. Z., & Sanders, D. B. 1987, in Interstellar Processes, ed. D. J. Hollenbach & H. A. Thronson (Dordrecht: Reidel), 21
 Spitzer, L. 1942, ApJ, 95, 329
 ———. 1978, Physical Processes in the Interstellar Medium (New York: John Wiley)
 Stark, A. A. 1984, ApJ, 281, 624
 van der Kruit, P. C. 1988, A&A, 192, 117
 van der Kruit, P. C., & Searle, L. 1981a, A&A, 95, 105
 ———. 1981b, A&A, 95, 116
 van Dokkum, P. G., Peletier, R. F., de Grijs, R., & Balcells, M. 1994, A&A, 286, 415
 Wainscoat, R. J., Freeman, K. C., & Hyland, A. R. 1989, ApJ, 337, 163
 Wilson, C. D., & Scoville, N. Z. 1990, ApJ, 363, 435